Qualification of the MMX Rover Locomotion Subsystem for the Martian Moon Phobos

S. Barthelmes, R. Bayer, W. Bertleff, M. Bihler, F. Buse, M. Chalon, G. Geyer, F. Hacker, C. Hofmann, R. Holderried, A. Kolb, E. Krämer, V. Langofer, R. Lichtenheldt, S. Moser, A. Fonseca Prince, K. Sasaki, H.-J. Sedlmayr, J. Skibbe, B. Vodermayer

Planetary rovers have proven their function and value for the Earth moon as well as Mars in the past decades. While these celestial bodies have a gravity of the same order of magnitude as the Earth, wheeled locomotion has never been performed on a body with much lower gravity. Within the Japanese Martian Moon eXploration (MMX) mission, a wheeled rover will land on the Martian Moon Phobos with a gravity of about 1/2000 of the Earth gravity. The Robotic and Mechatronics Center of the German Aerospace Center (DLR-RMC) has designed and built the locomotion subsystem (LSS) for this rover. As the first ever driving gear for milli-gravity, the LSS needed to undergo a comprehensive qualification campaign. Due to the very challenging timeline of this project, the extent of the campaign needed to be carefully tailored to the needs of the mission. This work describes the concept of the verification including some crucial tailoring choices that have been made. The individual domains of verification are then described in detail with their scope, setup, procedure and results. The goal of this publication is to give a good overview and a detailed insight into the verification of the LSS for milli-gravity. Besides follow-up missions to Phobos, this work is also a good foundation for the qualification of future driving gears for low gravity environments or small rovers in general.

S. Barthelmes et al., "Qualification of the MMX Rover Locomotion Subsystem for the Martian Moon Phobos," *2023 IEEE Aerospace Conference*, Big Sky, MT, USA, 2023, pp. 1-20, doi: 10.1109/AERO55745.2023.10115865

Qualification of the MMX Rover Locomotion Subsystem for the Martian Moon Phobos

Stefan Barthelmes[1] **Ralph Bayer**[2] **Wieland Bertleff**[2] **Markus Bihler**[2] **Fabian Buse**[1]
Stefan.Barthelmes@dlr.de

Maxime Chalon[2] **Günther Geyer**[2] **Franz Hacker**[2] **Cynthia Hofmann**[2] **Roman Holderried**[2]

Alexander Kolb[2] **Erich Krämer**[2] **Viktor Langofer**[2] **Roy Lichtenheldt**[1] **Sascha Moser**[2]

André Fonseca Prince[2] **Kaname Sasaki**[3] **Hans-Jürgen Sedlmayr**[2] **Juliane Skibbe**[1] **Bernhard Vodermayer**[2]

[1] German Aerospace Center (DLR)
Institute of System Dynamics and Control
Münchener Str. 20
82234 Weßling

[2] German Aerospace Center (DLR)
Institute of Robotics and Mechatronics
Münchener Str. 20
82234 Weßling

[3] German Aerospace Center (DLR)
Institute of Space Systems
Robert-Hooke-Str. 7
28359 Bremen

Abstract—**Planetary rovers have proven their function and value for the Earth moon as well as Mars in the past decades. While these celestial bodies have a gravity of the same order of magnitude as the Earth, wheeled locomotion has never been performed on a body with much lower gravity. Within the Japanese Martian Moon eXploration (MMX) mission, a wheeled rover will land on the Martian Moon Phobos with a gravity of about 1/2000 of the Earth gravity. The Robotic and Mechatronics Center of the German Aerospace Center (DLR-RMC) has designed and built the locomotion subsystem (LSS) for this rover. As the first ever driving gear for milli-gravity, the LSS needed to undergo a comprehensive qualification campaign. Due to the very challenging timeline of this project, the extent of the campaign needed to be carefully tailored to the needs of the mission.**

This work describes the concept of the verification including some crucial tailoring choices that have been made. The individual domains of verification are then described in detail with their scope, setup, procedure and results. The goal of this publication is to give a good overview and a detailed insight into the verification of the LSS for milli-gravity. Besides follow-up missions to Phobos, this work is also a good foundation for the qualification of future driving gears for low gravity environments or small rovers in general.

TABLE OF CONTENTS

978-1-6654-9032-0/23/$31.00 ©2023 IEEE

1. INTRODUCTION

Wheeled mobile robots have proven to be very valuable for space exploration since they increase the action radius of a lander without the cost and risk of a human mission. The French Centre National d'Études Spatiales (CNES) and the German Aerospace Center (DLR) jointly develop a 20kg rover for the Martian Moon eXploration (MMX) Mission of the Japanese Space Agency (JAXA). The launch is scheduled for 2024 and the rover will be deployed on Phobos in the first half of 2027.

The Robotics and Mechatronics Center of DLR (DLR-RMC) develops and builds the locomotion subsystem (LSS) for this rover. It consists mainly of four shoulders, legs and wheels, four hold-down-and-release mechanisms (HDRM), an electronic box and software, see Figure 1. The detailed design of the prototype and flight model (FM) have been presented at previous IEEE Aerospace Conferences in 2020 [1] and 2022 [2], respectively, and will thus not be repeated in detail here.

This publication presents the qualification campaign of the LSS in detail. Overall, the LSS is qualified as a subsystem, meaning that most of the tests and analysis were performed on a fully assembled LSS and not for individual components and processes. The main test campaign took place between January and June 2022 and consisted of about 150 days in test laboratories for qualification and acceptance testing. For some crucial parts, a separate testing or analysis was performed, such as the hall effect sensors, glues and the wheels. There were many more tests with the engineering model (see [2]) but this paper focuses on the qualification, i.e. the tests and analyses that are used to justify compliance to the requirements. Although the LSS was qualified specifically with respect to the requirements of the MMX Rover mission, many aspects can be transferred to other missions with a similar profile, including

- deep space planetary exploration mission with large temperature variation and low gravity

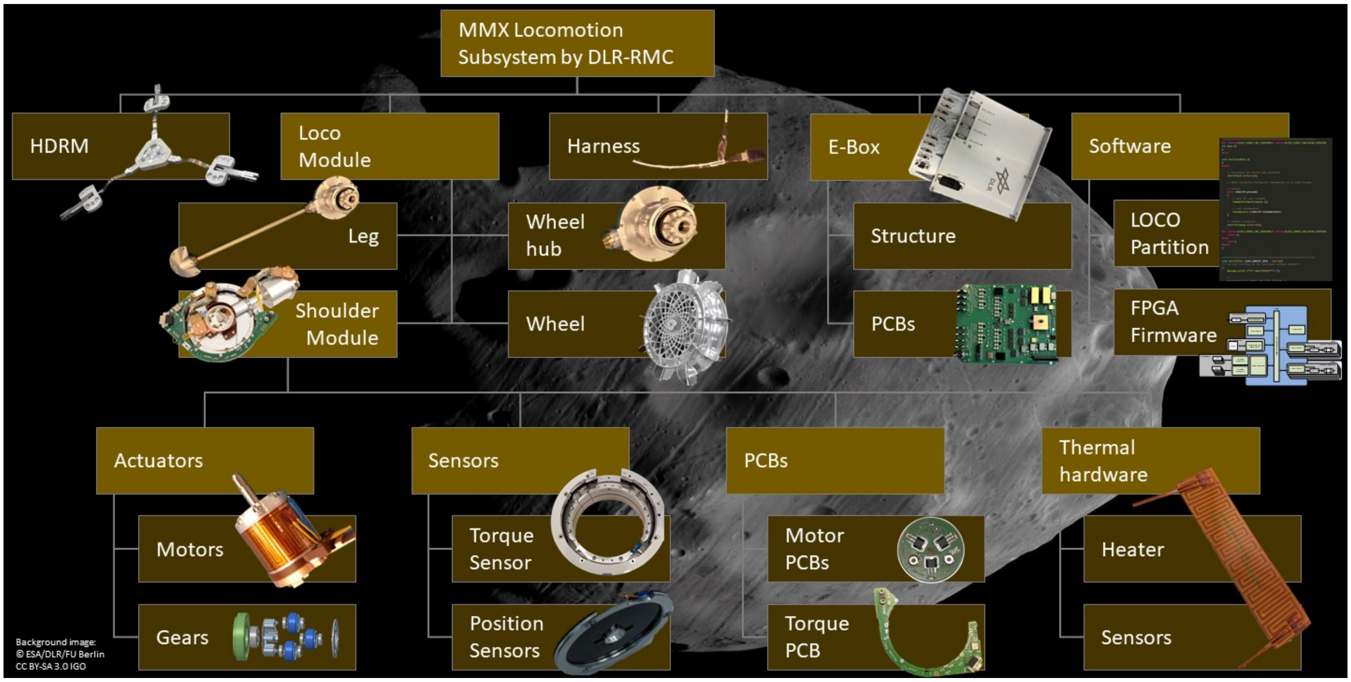

Figure 1. Product tree of the LSS.

- relatively low radiation exposure for a deep space mission
- high mechanical loads due to the launcher and a non-decelerated impact on the surface

The work is organized as follows: The overall verification strategy and the functional test are described in Sections 2 and 3, respectively. The further sections present the verification by domains, mostly in chronological order. The inspection of the subsystem and a burn-in of the E-Box are described in Section 4. After these first preparatory aspects, the environmental verification follows, divided into mechanical (Section 5), thermal (Section 6) and electromagnetic compatibility tests (Section 7). The functionality and performance verification of the LSS are described in Sections 3 and 8, respectively. In Section 9, the verification of the required lifetime is described. The software verification is summarized in Section 10. Section 11 details the mentioned tests on component level that complement the LSS qualification campaign.

2. VERIFICATION STRATEGY

The goal of the verification is to prove compliance to the specifications, i.e. the requirements that are applicable to the LSS. In the following subsections, some general choices for the LSS verification are summarized, tailoring choices are described and the overall test schedule, as well as organizational aspects are shown.

Component / Sub-Assembly Heritage

Whenever possible, components have been procured that are fully qualified for the expected environment, such as the field programmable gate array (FPGA), memory devices, analog-to-digital converters (ADC), analog integrated circuits (IC) to name just some of them. If components were not available with the required qualification status, delta-qualification has been performed (see Section 11).

However, none of the sub-assemblies of the LSS have been pre-qualified to the expected environment. For some sub-assemblies, like the torque and position sensors as well as rotor and stator, heritage from previous projects exists. Others, like the wheel, the firmware and software and the HDRM are entirely new developments. Due to this limited heritage for the relevant environment on sub-assembly level, all of them need full qualification.

Verification Level

Verification of a subsystem can be performed purely on LSS level after full integration or additionally on lower level, such as single component or sub-assembly level. The more verification on lower level is performed, the less risky the approach, as verification problems are identified early. While some subsystem level verification can be spared in this case, some tests are still necessary for proving full subsystem functionality. Additionally, verification on lower level usually implies more effort, costs and time between design freeze (at least of the sub-assemblies) and the delivery of the flight hardware. The verification strategy of course needs to meet given boundary conditions, such as delivery deadlines, given requirements regarding qualification and acceptance testing and resource constraints. As a result, due to the very tight schedule and given need dates, the qualification of the LSS is mostly performed on subsystem level with the exception of some critical components described in Section 11.

Verification Models

Two different approaches can be followed for the qualification and flight model.

In the qualification model (QM)+ flight model (FM) approach, two separate but as identical as possible models are built. The QM is used for the qualification tests with qualification loads, resulting in high stress for the hardware. The FM is tested with lower acceptance loads to check the representativity of the QM and proper built quality of the FM.

Table 1. Verification methods according to ECSS.

Method	Description
Review of Design	Use approved records or evidence that unambiguously show that the requirement is met.
Analysis	Perform theoretical or empirical evaluation, such as for example simulation.
Inspection	Determine of physical characteristics by visual inspection or measurement.
Test	Measure product performance and functions under representative simulated environments.

Generally, not all qualification tests need to be done on a QM. If anoter model is used it must be representative in terms of the aspects to be tested in the respective test. Since most subassemblies of the LSS evolved until the QM and FM design (see [2]), most of the LSS qualification tests require the QM. Rare exceptions are the sealing concept of the shoulder and the wheel design, see Sections 5 and 11.

For extremely tight project schedules, a proto-flight approach (PFM) can be followed. This means that one flight representative model is built (the PFM) and used for qualification and the flight. To not stress the flight hardware too much before launch, qualification loads but only acceptance duration is used. However, the PFM approach still implies more stress of the flight hardware. Additionally, there is no possibility to react if problems are seen, whereas for the QM+FM approach the FM can still be changed (very limited) in case of major problems on the QM.

For these reasons and due to the novelty of the LSS, the QM+FM approach is chosen for the LSS qualification campaign although the PFM apporach is pursued for the full rover.

The E-Box and the locomotion modules are mostly tested separately for two reasons: Firstly, the environments are very different since the E-Box is in the thermally insulated and mechanically damped inner compartment of the rover. Secondly, the integration of E-Box and modules are performed in different locations at different points in time, thus the need dates differ. Decoupling the test campaigns so reduces complexity of the test setups and schedule dependencies.

Verification Methods

Verification methods according to ECSS-E-ST-10-02C are described in Table 1.

For some environmental requirements, analysis- or test-based verification is acceptable in the project. A finite element model for modal analysis and a detailed thermal model were used for the design and development of the LSS. The mechanical design of the LSS allows sliding and gapping at the HDRM interface and the thermal coupling varies largely with part tolerances and assembly, which makes the numerical simulation very complex [3]. Therefore, the analysis was only used for the design phase, while the qualification of the LSS relies on tests for the environmental requirements.

Verification Control

For verification control, a Requirements Verification and Compliance Matrix (RVCM) is used. The RVCM lists all requirements applicable to the subsystem, and for each requirement:

- the project milestone for which the verification is due
- the model used for the verification
- the related requirements (upstream and downstream)
- the compliance status (compliant, partially compliant, not compliant)
- the compliance justification including references to related documents
- the final verification status (open, closed, partial)

The RVCM is extended with macros to select all requirements that are relevant for a specific test. This enables the test responsible to easily see all requirements that need to be respected or verified and also makes it easier to ensure that all requirements are covered.

Table 2. Main General Rover and Product Assurance Requirements

No.	Requirement
R1	Mass & Power Budget
R2	Thermal Control Requirement
R3	Lifetime of the Rover
R4	Requirements for Documentation & Verification

Requirements for Verification

The requirements for the locomotion subsystem of the MMX Rover are structured in

- General rover requirements
  - Mechanical, thermal and electrical requirements
  - Assembly, integration and testing (AIT) requirements
- Product and Quality Assurance Requirements
  - Requirements for materials and processes
  - Requirements for qualification, acceptance and screening
  - Requirements for electronic, electrical and electromechanical (EEE) parts
  - Requirements for printed circuit boards (PCB) manufacturing and soldering
- Subsystem requirements
  - LSS functional, performance & operational requirements
  - LSS Design and Interface requirements
  - Additional environmental and test requirements for LSS

The requirements are either tailored from ECSS, directly refer to ECSS or are written specifically for the MMX Rover Mission. No exhaustive list of all requirements is provided here, as this would exceed the scope of this paper. The main requirements driving the mechanical, thermal, electrical, performance and operational verification testing are listed in Tables 3, 5, 6, 8 and 11 and Figure 12 and Table 13 in the respective section. The main general rover and the main product assurance requirements driving the verification are listed in Table 2.

Functionality, Performance and Degradation Evaluation

The evaluation of functionality and performance is essential for the verification. According to ECSS, two performance tests, one before and one after the environmental tests allows to guarantee the system performance in spite of the stress of environmental conditions. For the LSS, the scope of the performance test is divided into two sub-scopes: Firstly, the

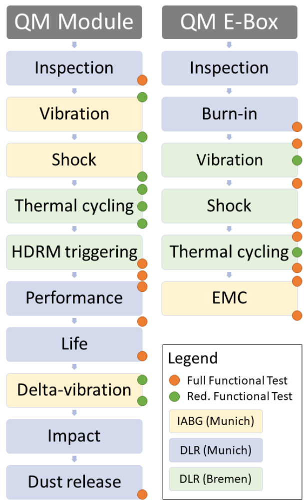

Figure 2. Qualification Test Sequence.

absolute performance of the subsystem needs to be proven. Secondly, a potential performance degradation of the subsystem due to the environmental tests needs to be detected.

Due to the complexity of the performance test (PT) for the LSS and the quantitativeness of the functional tests (FT), the ECSS is tailored. The degradation is assessed with the FT after each environmental test and even after transporting the subsystem. Only one PT is performed at the very end of the environmental tests to verify the absolute performance requirements, such as the maximum load torque for the drives. With the many FTs performed, this approach allows a much more detailed assessment of when a potential degradation happens, while sparing the costs and time of one PT.

Qualification Test Program & Organization

The project schedule requires parallel qualification and acceptance testing and the E-Box and modules are tested separately as justified above. These choices lead to more organizational complexity since there are four independent test campaigns and, at times, four parallel tests in different locations. So, a very detailed resource planning, regarding time, test personnel, test equipment and test facilities is required.

The qualification test sequence is derived from project requirements and ECSS and is summarized in Figure 2.

Additionally, inspection of optical properties, labeling, documentation and physical properties is done.

Test readiness and post test reviews are organized before and after each test. The review committee consists of

- LSS responsible
- LSS test responsible
- LSS product assurance
- Rover product assurance
- Rover verification responsible
- Rover architect/system engineer responsible for the requirements that are subject to be verified in the respective test

The purpose of the test readiness review is to ensure availability and suitability of the test facility, availability of the device under test and needed ground support equipment as well as the availability and correctness of all needed documentation and the absence of blocking non-compliance. Its formal outcome is the release of the test.

Post test reviews take place after each test to summarize and review the test sequence, deviations and main results. The formal outcome of these reviews is a decision if the test campaign can be continued and if non-compliance reports need to be issued.

3. FUNCTIONAL TESTS

Functional tests are performed before and after all environmental tests, as well as at the beginning and at the end of the campaign and after transports as can be seen in Figure 2. The extensive telemetry data that is acquired during functional tests allows to assess degradation and therefore partly serves performance test needs, see Section 2 for details.

Scope

The aim of the functional tests is to confirm that the LSS hardware modules are fully operational as required. This includes the wheel and leg drive trains as well as position, torque, acceleration, gyroscope, temperature, radiation, current and voltage sensors.

For all functional tests, the same software and a proprietary communication bridge is used to send commands to the LSS hardware and receive sensor data from it. The bridge converts between SpaceWire (the communication interface of the E-Box) and a universal asynchronous receiver transmitter (UART) device that is connected to a standard computer. This UART device is used by the functional test software to communicate with the E-Box, which allows to send commands and log all telemetry data during functional tests.

The software is configurable and adaptable to allow testing with the different setups for the all the E-Box and module qualification tests. During the shaker tests of the shoulders, for example, the wheels and legs are fixed and no movement can be performed. To account for these restrictions, the software is split into several sub-tests, which can be executed in any combination, depending on the hardware setup. For all sub-tests, pass criteria with quantitative thresholds are defined to decide whether a sub-test is successful and to assess objectively if there is any degradation. The most important sub-tests are:

- The passive health check verifies that all sensor inputs (voltage levels, temperatures, etc.) are in an expected range.
- The large movement check moves the leg and wheel motors to verify the functionality of all involved parts from the motor inverter to the mechanical gears of the wheels and legs.
- The micro movement check allows to test the wheel and leg motors and electronics even in the locked configuration. The motors are therefore commanded such that the wheel/shoulder rotation would be $< 0.03°$, however, this is less than the gear backlash.
- The position sensor check validates the leg potentiometers by performing one or more full rotations of the leg while recording the sensor data.
- The torque sensor check validates the shoulders' torque sensors by recording a manually applied torque in each direction.

In Section 2, the FFT and RFT were introduced. The FFT comprises all sub-tests from above, whereas the RFT only contains the sub-tests without movement of the legs and wheels, e.g. due to locked HDRMs (RFT). Therefore, the large movement check and the position sensor check are not included in the RFT.

E-Box FFT: setup and procedure

For the E-Box FFT, all motors and sensors must be connected to the QM E-Box. However, it is not required to connect the actual QM motors and sensors since the test is about the internals of the E-Box itself. Therefore, compatible EM or prototype motors and sensor dummies are used instead.

For most qualification tests, the test setups are already sufficient to perform an E-Box FFT without restrictions. Exceptions are the mechanical tests, where no cables are attached to the E-Box during the vibration and shock. Therefore, the motors and sensors have to be connected to the E-Box for the conduction of the FFT, which is only done before and after all axes to spare connection cycles.

E-Box FFT: results

All tests of the E-Box FFTs during the qualification campaign are passed and the results show no degradation of the electronics. Deviations are related to issues with the ground support equipment or the test software, not to the QM E-Box. For example, the temperature sensor inside an EM motor is damaged during thermal tests. By swapping the motor in question with an operational one, it is verified that the QM E-Box has no issues.

Module FFT: setup and procedure

For the module FFTs, the QM shoulders are connected to an EM E-Box so that the test computer can send commands and log sensor data. Similar to the E-Box FFTs, most test setups fulfill the requirements for a shoulder FFT with the exception of mechanical tests. However, the modules are in locked configuration throughout mechanical and thermal testing, therefore no movement is allowed and only RFTs can be performed.

Module FFT: results

The failures that are detected with the RFT and FFT are described in more detail in their respective section. These are the torque sensor failure after re-applying the vibration qualification loads on QM2 a second time (see Section 5) and the foil potentiometer non-compliance in cold conditions (see Section 6). Note that the FFT with its active torque sensor check and detailed data analysis enabled to discover the failures immediately and assign them to a specific test. With a passive functional test and only active performance tests at the beginning and end of the test campaign, it would not be clear when the failures happened.

All other functional tests of the qualification campaign are passed and, as described in the respective sections, the seen non-compliances were all accepted. Comparing the logged telemetry data of all performed shoulder FFTs shows that the mechanics and electronics suffered no degradation.

As an example, Figure 3 shows the current of a wheel motor during the large movement checks over the qualification campaign. Note that the temperatures in the legend concern the chassis interface of the shoulder (TRP1, see Section 6). The motors and shoulder electronics where at the same minimum operational temperature of $-35\,^{\circ}\mathrm{C}$ for both cold cases. The success criteria for the large movement check define a margin

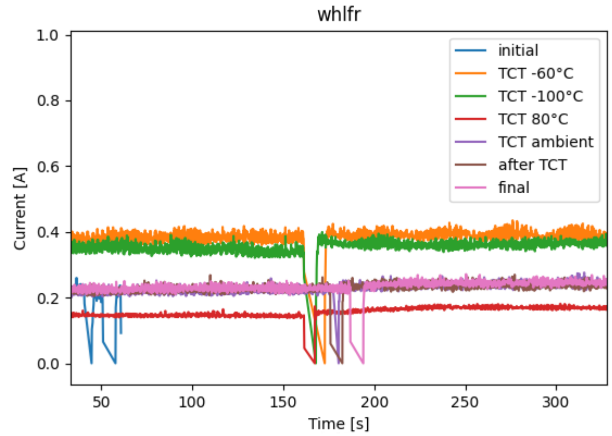

Figure 3. Phase current of a wheel motor through the qualification campaign.

of three to the maximum phase current of the motor. With a maximum current of $4.5\,\mathrm{A}$, the motor phase current shall not exceed $1.5\,\mathrm{A}$. Also, the average phase current of the motor before and after the qualification campaign shall not change by more than $20\,\%$ under comparable conditions. At ambient temperature, the motor phase current in Figure 3 shows no significant change and stays well below $1.5\,\mathrm{A}$ with a margin to the maximum current of more than 15. As expected, during the thermal tests a higher motor current can be observed at lower temperatures (green and orange lines) and vice versa (red line), always remaining well below $1.5\,\mathrm{A}$.

The initial shoulder FFTs after the burn-in test showed a non-compliance with one of the potentiometers in the shoulders. The measured voltage deviated from the expected value by a large amount in some positions and the delta was changing significantly over the measurement range of the sensor. An NCR was raised to track the issue and an inspection of the affected shoulder showed that mechanical tensions in the structure of the potentiometer, probably caused by differences in the thermoelasticity of various components, were the source of the problem. The sensor was repaired and a repeated shoulder FFT showed that sensor is working as expected. To avoid the same issue in the FM shoulders, the assembly procedure of the sensor is adapted.

4. Inspection and burn-in test

Scope

The inspection and burn-in test of the LSS are carried out in order to verify the quality of the workmanship and to identify defect or low quality parts. Multiple requirements for screening, component quality, physical properties and spin-in of commercial off-the-shelf (COTS) parts are the basics of the four-fold LSS inspection strategy.

Key inspection points (KIP) are performed after each important step in the manufacturing process. A main inspection, including physical properties measurement and inspection of the completeness of the sub-assembly, is done before the QM enters the test sequence. Before and after tests, the LSS is subject to optical inspections to detect possible damages in the system due to the test loads. Before the delivery to the system, an outgoing inspection is performed to check and document the final state of the subsystem.

All these steps are performed with the QM of the LSS, in order to guarantee an error free model and optimize the processes for the FM.

Setup and Procedure

The burn-in was only performed with the locomotion E-Box, whereas the locomotion modules were tested during the run-in period as part of the manufacturing and integration process. Based on MMX requirements, the test was performed in accordance with MIL-STD-883 Rev. L [4] in a thermal chamber within a clean room. During the test, the E-Box was powered within its rated limits and operated in active stand-by mode at $85\,°\mathrm{C}$ environmental temperature for $100\,\mathrm{h}$ without applying vacuum or heavy load on the electronics. In the active stand-by mode, the system is running and reading all sensors regularly, but is not operating the motors. The latter were driven once per hour for one minute in order to limit the load. Housekeeping data and power supply data (currents and voltages) are recorded regularly in order to verify the proper operation of the E-Box. In addition, the temperature is recorded with an external measurement system. The setup and all parameters were defined during the test preparation and accepted in the test readiness review (TRR).

Results

During multiple inspections, which were conducted as part of the manufacturing and assembly process, a few non-compliances were found and reported with non-conformance reports (NCR). This was done in order to ensure a tracking process which supervises the corrections of the defects. Minor deficiencies were corrected right away and reported accordingly. In the main inspection, the LSS was found to be within its volume and mass budget and compliant to the requirements.

During the burn-in process, no errors were detected and the E-Box performed nominally. All supply currents stayed within the rated limits and no functional interrupt was reported during the $100\,\mathrm{h}$ operation and the burn-in test was concluded successful in its post test review.

5. MECHANICAL VERIFICATION

The mechanical qualification campaign of the LSS is conducted in several tests: The resilience to vibration, shock and ballistic loads as well as the reliability of the HDRM releases. Between each test case, full functional tests (or RFTs when the HDRMs are locked) ensure that the system performs nominally. In particular, the drive trains and sensors are checked, to ensure that any degradation would be detected immediately and traced back to the test case easily, see Sections 2 and 3. A more detailed view of the mechanical design of the LSS, as well as of the test campaigns, can be found in [3].

Scope

One common hardware setup is designed to match the interfaces across the test facilities in order to maintain the DUT (device under test) configurations between the different tests. However, two different variants of the setup are used, because only one representative chassis side plate was available for the LSS tests. This also allows to cover a wider range of mechanical and thermal behavior than using only one variation and thereby minimizes the risk that the system level predictions are too conservative (or not conservative enough). The variants are named QM1 and QM2: QM1 consists of two left locomotion modules mounted into the representative chassis side panel (aluminum honeycomb / carbon sandwich) [3], as depicted in Figure 4. In contrast, QM2 are two right locomotion modules in an aluminum dummy of the chassis side panel, which is black anodized for the thermal test from Section 6. In the following, a brief summary of the setup, procedure and results are given for the dedicated tests in order to verify the requirements.

Table 3. Main locomotion module vibration and shock requirements.

N°	Requirement
R5	The LSS shall withstand sinus test levels
R6	The LSS shall withstand random test levels
R7	The LSS shall withstand shock test levels
R8	The frequency shift shall be less than $5\,\%$ and the amplitude shift less than $20\,\%$ for modes with an effective mass greater than $10\,\%$

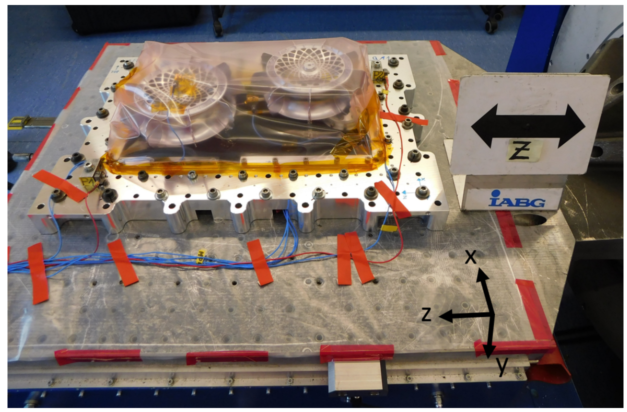

Figure 4. Hardware setup on the shaker.

Vibration and Shock Test: Setup and Procedure

The launch of the rocket induces significant vibrations and shocks to the entire rover. To ensure that the locomotion modules survive the launch and is still operational, Finite Element simulations were carried out during the development. However, the qualification relies on vibration and shock tests as justified in Section 2. The main requirements to be verified on the shaker and shock plate are summarized in Table 3.

As previously described, two hardware setups are utilized. Primarily due to the different panels and their stiffness properties, individual loads for each configuration are derived by the rover system team. The sine, random and shock levels used for the qualification are specified for each setup in Table 4.

The setups (see Figure 4) are equipped with accelerometers at the locations that showed resonance frequencies with more than $10\,\%$ of the effective mass as obtained by a detailed modal analysis of the LSS. The setups are screwed to the shaker interface plate of the facility in the appropriate axis direction as shown in Figure 4 and are excited with sine and random loads for each axis. In order to detect any possible degradation of the DUT, the resonance profile of the setup is checked before and after each axis excitation.

Subsequently, the setups are transferred to the shock facility

Table 4. Vibration and shock loads for QM1 and QM2.

Frequency (Hz)	Sinus-X (g)		Sinus-Y (g)		Sinus-Z (g)	
	QM1	QM2	QM1	QM2	QM1	QM2
5-24	11mm(0-peak)		11mm(0-peak)		11mm(0-peak)	
24-100	26		26		26	
Sweep rate (oct/min)	2		2		2	
Frequency (Hz)	Random-X (g)		Random-Y (g)		Random-Z (g)	
	QM1	QM2	QM1	QM2	QM1	QM2
20	0.02	0.02	0.001	0.001	0.001	0.001
100	0.25	0.265	0.075	0.075	0.04	0.04
145	-	-	0.075	0.075	-	-
170	-	-	-	-	0.04	0.04
175	-	-	0.22	0.36	-	-
200	-	-	-	-	0.15	0.14
230	-	-	0.22	0.36	-	-
260	-	-	0.075	-	-	-
270	-	-	-	0.14	-	-
330	-	-	-	-	0.15	0.14
370	-	-	-	-	0.075	-
380	-	-	-	-	-	0.04
420	-	-	-	0.14	-	-
460	0.25	0.265	-	-	-	-
500	0.45	0.465	-	0.71	-	-
620	-	-	-	-	0.075	0.04
640	0.45	0.465	-	-	-	-
670	-	-	-	-	0.14	0.08
680	-	-	0.075	-	-	-
710	1.05	1.125	-	-	-	-
720	-	-	0.13	-	-	-
820	-	-	-	0.71	-	-
870	-	-	0.13	-	-	-
880	-	-	-	-	0.14	-
900	-	-	-	-	-	0.08
920	1.05	1.125	-	-	-	-
2000	0.001	0.001	0.0015	0.0015	0.001	0.00035
gRMS (1σ)	23.83	24.54	10.29	21.98	10.39	8.36
Duration (s)	120		120		120	
Frequency (Hz)	Shock-X (g)		Shock-Y (g)		Shock-Z (g)	
	QM1	QM2	QM1	QM2	QM1	QM2
100	20		20		20	
1000	1000		1000		1000	
10000	1000		1000		1000	

and equipped with new acceleration sensors. According to Table 4, each setup is submitted to the given levels three times.

Finally, a last resonance profile and an RFT guarantees that the DUT is functional within the limits of the launch locked configuration.

Vibration and Shock Test: Results

The requirements of frequency and phase shift cannot be met, as expected from tests with the engineering model. The deviation is due to the design principle of the HDRM and was rated acceptable after the engineering model tests. Furthermore, during the acceptance y-axis vibration of the flight model, a non-conformance between the qualification model and the flight model resonance at 270 Hz, as shown in Figure 5, was reported. The flight model and the modal analysis show a distinctive peak at 270 Hz, whereas the qualification model showed a negligible amplitude at this frequency. To also qualify the configuration which shows the peak at 270 Hz, a third test (delta qualification test) with the hardware setup QM2 is performed, since it is the closest to the flight model. The frequency in question could be reproduced with this setup and a slightly adapted assembly procedure before conducting the second full vibration qualification on the QM2 setup. The delta qualification thereby also allows to improve the assembly procedure by adding steps for aligning the deployable part with the load carrying part of the HDRM during the fixture of legs and wheels in their launch lock position.

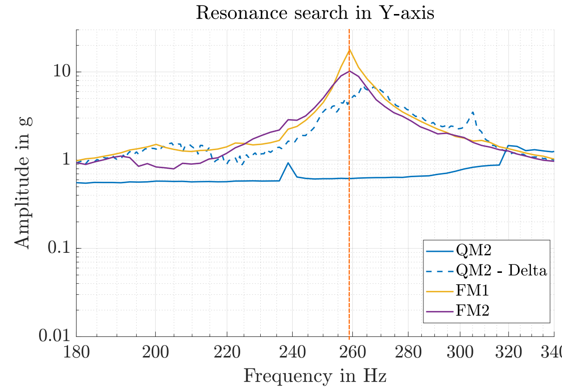

Figure 5. Discrepancy at resonance frequency of 270 Hz in y-axis between qualification and flight model

Overall, the variation and shifts in eigenfrequencies are explainable but could not be considered in the locomotion and full rover analysis. This yields a risk that the mechanical environment that was provided for the LSS qualification is not conservative enough. To finally confirm resilience to the mechanical loads of the LSS within the full rover, the planned vibration test on rover level is thus particularly important also for the LSS.

After the second qualification test of the QM2 setup, a defect in both torque sensors is observed. It is found that the torque sensor bodies have no structural damage and the harnesses are still electrically connected to the strain gauges. After disassembly and microscopic analysis, the defects are traced down to an internal damage in the applied strain gauges. Therefore, an extended torque sensor test is introduced to the FM acceptance test campaign to check the integrity of its torque sensors, which showed no signs of defects until the end of the acceptance campaign. It shall be noted that the torque sensor will only be used to further reduce the risk of damaging parts in the situation of a blocked LSS. Nevertheless, the impact of a hypothetical torque sensor failure on the FM was discussed with the rover responsible. A strain gauge failure only leads to a reduction of the anomaly detection capabilities and is therefore found to be acceptable.

Ballistic Impact Test: Setup and Procedure

During landing, the LSS can be the first impact point as it covers a large fraction of the exposed surface of the rover. It is expected that the rover is dropped from about 50 m above the Phobos surface, which results in an impact velocity of around $0.9\,\mathrm{m\,s^{-1}}$. The expected impact energy sums up to 10.1 J, which needs to be withstood by the mechanical structure of the LSS. Moreover, regolith may contaminate the outer surfaces and hinder the functionality of the HDRM. Table 5 summarizes the main requirements to be resilient against the ballistic impact, contamination by regolith and thermal load.

The hardware setup QM2 is selected for the ballistic impact test and it is done after the nominal qualification sequence since it could not be done in the clean room. At first, one of the wheels is charged at room temperature with a falling weight of 4 kg from a height of 25 cm, which corresponds to the worst-case impact expected on Phobos. Subsequently, the HDRM and leg structure of the tested locomotion module is contaminated with dust from 40 µm up to few mm (following

Figure 6. Images of the impact (left), dust (top right) and release (bottom right) test sequence. This was performed at the end of the nominal qualification sequence since it could not be done in the clean room.

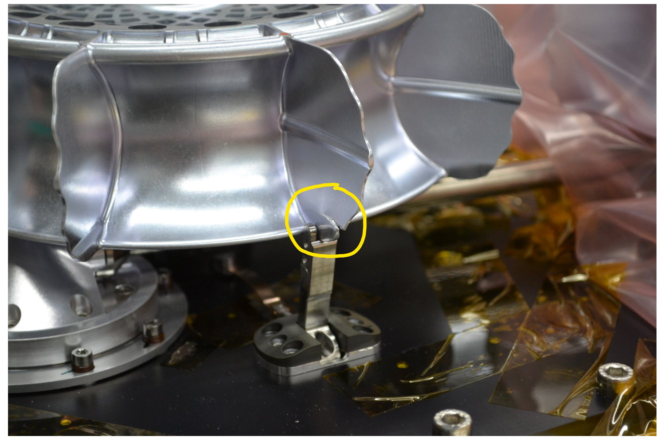

Figure 7. Non-impairing damage on one wheel grouser of the locomotion module tested at ambient.

the expected regolith particle size provided in the Environment Requirement Document of the project). Subsequently, the release of the HDRM is triggered, see the full process in Figure 6.

The procedure is repeated for the second locomotion module of the hardware setup QM2 with the important distinction that the second module is additionally cooled down to $-125\,^{\circ}\mathrm{C}$ to perform the cold impact, contamination and release.

Ballistic Impact Test: Results

The ballistic impact test with contamination, thermal load and the final HDRM release were successful for both locomotion modules. The only damage is observed in the locomotion module tested at ambient, which revealed a tear at the wheel grouser, directly below the collision point as shown in Figure 7. Such a damage in the wheel structure was expected by design for certain impact situations and the functionality is not hindered in any way. Functional tests (see Section 3) confirm that the LSS's full functionality. Also, the disassembly of the modules verified the sealing concept to be successful at both thermal scenarios.

E-Box Vibration and Shock Testing

The E-Box is also subjected to a vibration and shock test. Due to its location inside the damped inner part of the MMX Rover, the shock and vibration levels for the E-Box differ in contrast to those of the locomotion module tests. Differences in the results of the low eigenfrequencies between QM and FM/FS lead to the need for a delta-qualification with the FS model. The cause for these differences turned out to be a mechanical gap in the housing, resulting from a thickness variation of the electronic boards (PCBs). The slightly thicker of the two PCBs led to a small gap in the housing and therefore changed the eigenfrequency of the whole E-Box.

Table 5. Main ballistic impact requirements.

N°	Requirement
R9	The LSS functionality shall not be impaired by regolith contamination
R10	The LSS shall remain nominally functional after the expected impact on Phobos
R11	The LSS shall prevent dust contamination inside the rover

All functional tests were successful. A non-compliance about the lowest eigenfrequency being slightly below the required $300\,\mathrm{Hz}$ was accepted due to a very limited risk for the rover.

6. Thermal Verification

During the qualification of the LSS, two temperature cycling tests are performed inside a thermal vacuum chamber (TVC). One test is done with the locomotion modules including the corresponding HDRMs, while the other test focuses on the locomotion E-Box. The main reasons for the separation are that different temperature ranges have to be reached within nine cycles. Also, a combined test would increase the complexity of the setup and limit the workspace of the locomotion modules during the functional tests (see Section 2).

Scope

There are two main verification parts of the thermal cycling test: The first is to validate the resilience to the expected thermal environment and the second is to verify the functionality of the LSS at minimum and maximum operation temperatures. Besides the operation of the motors and the reading of the sensors, this includes the releasing of the HDRMs.

Furthermore, thermal balance tests are performed on both components to correlate thermal analysis models, leading to more accurate predictions of the thermal behavior for the cruise and Phobos mission phase.

Modules thermal cycling test: setup and procedure

The main requirements for the locomotion modules thermal cycling qualification test are listed in Table 6.

Figure 8 shows the mechanical setup inside the TVC. Only the QM1 setup (the one with the representative chassis side panel, see Section 5) allows to verify the HDRM release functionalities due to thermoelastic representativity. Two cameras together with a light bulb enable the visual inspection after the HDRM release during the ninth cycle.

The entire test setup, including power supplies and data ac-

Table 6. Requirements for the Locmotion Module QM thermal cycling test.

No.	Requirement
R12-14	Compliant to temperature stability & rate of change, vacuum pressure level.
R15-17	Functional tests successfully performed.
R18	HDRM successfully released.
R19	Cruise heating line is electrically connected.
R20	Phobos heating line is functional.
R21	Integrity of internal temperature sensors verified.
R22	Full performance of internal temperature sensors checked.

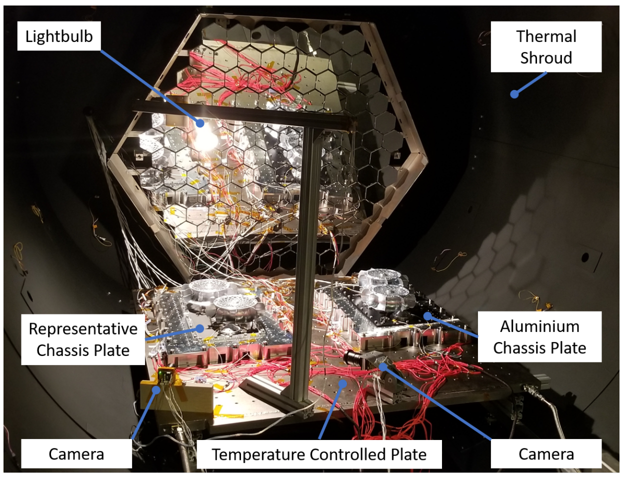

Figure 8. Locomotion modules inside the TVC.

quisition devices, is controlled by dedicated software running on a test laptop. The latter is also used to record all relevant data, such as temperature sensor readings, power values and the housekeeping data. This data is provided by the E-Box that, in this test, serves as ground support equipment (GSE) to drive the locomotion modules.

The two temperature reference points (TRPs), that have been defined for the locomotion modules, are controlled independently for each module during the test. TRP1 is defined on the outside of the chassis plate close to the locomotion shoulder (see Figure 9). TRP2 is close to the electronic components within the shoulder module, such as the joint torque sensor PCB and the motors. The thermal design of the locomotion modules allows to heat up the electronic components independently during the mission due to the shoulder being thermally isolated from the chassis plate and equipped with heat foils (see [2] for details).

Since a reliable temperature control of the TRP2 is crucial to prevent too low temperatures of the electronics, a heater controller is designed to control all four shoulder heaters independently from each other. For data acquisition and parameterization, it is connected to the test control software. However, it works independently such that the TRP2 temperature can be kept in the desired range even in case of a software failure on the test laptop or a disconnection. It also features an additional open loop mode as fallback for each channel, which allows continuation of the test even for temperature sensor failure.

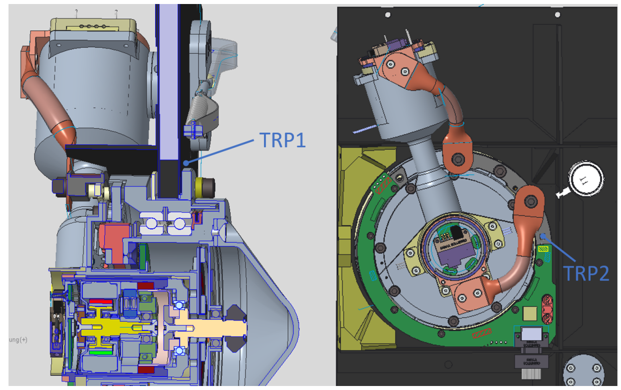

Figure 9. Temperature Reference Points of the locomotion modules.

Table 7. TRP1 and TRP2 qualification temperatures for locomotion modules. The $()^*$ indicates temperatures that were varied for the four QM modules.

LSS state	TRP1 [°C] min	TRP1 [°C] max	TRP2 [°C] min	TRP2 [°C] max
non OP	−125	+85	−80*	+85
OP Phobos	−100*	+70	−35	+80
OP Cruise	−125	+70	−35	+70
HDRM release	−110	+70	−35	+70

The thermal environment for the locomotion modules is very challenging, therefore great effort was made to improve the thermal design (see [2]). Despite these improvements, the environment is still challenging, which is why the four QM modules have been used to test different temperature combinations of the cold case. The temperatures that are given in Table 7 represent the qualification environment as required from the thermal analysis of the rover. One module, which hence represents the actual qualification module, is subject to the full temperature range. The other three modules are tested at different variations of the temperatures with an asterisk in Table 7. These relaxed temperature levels reflect the minimum mission success on one side and also more heating of the locomotion shoulders on the other side. With this strategy, a potential degradation of the actual qualification model at the worst conditions could be compared to the other modules with the relaxed temperatures. This can help for the operations strategy, however, no degradation was seen even for the worst conditions, as will be detailed in the results section.

The TRP1 temperatures have been cycled as a "touch-and-go" target, i.e. without a dwell time, in order to achieve a time-efficient test duration. A dwell time for TRP1 is only satisfied in the ninth cycle for HDRM release triggering and in all subsequent functional tests. The rationale is that most of the mechatronic components (except for the strain gauges and the position sensors) are thermally close to the TRP2 zone where the dwell time requirement is always met. It is therefore acceptable to only respect a dwell time in the said cases.

Modules thermal cycling test: results

For the requirements R15-17, which are the pass fail criteria for the functional test (see Table 6 and Section 3), the test is partially passed: The foil potentiometer of all four shoulders

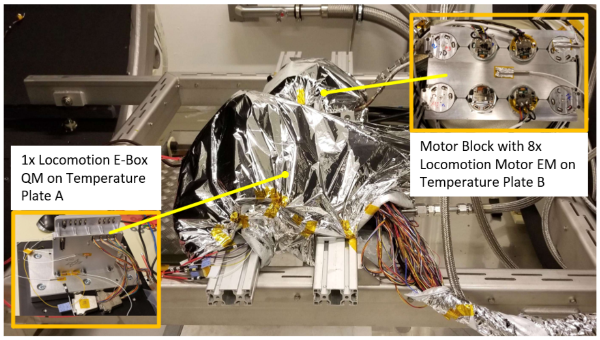

Figure 10. Locomotion E-Box inside the TVC.

Table 8. Requirements for the locomotion E-Box thermal cycling test.

No.	Requirement
R23-26	Compliant to temperature stability & rate of change, vacuum pressure level.
R27	Functional tests successfully performed.
R28	$1\,\mathrm{h}$ continuous operation successful.

shows discontinuous measurements during the TVC cycles and also in the functionality tests for cold temperatures. Furthermore, for one module, the micro movement fails on one motor due to a grounding problem with the EGSE harness, which connects the E-Box with the locomotion modules. This is verified with one test with open chamber but still the same harness and one test with shorter harness (close to the flight one) outside the TVC after the TCT. The problem persists for the open chamber but vanishes with the shorter harness and it can thus be clearly associated with the GSE, rather than a non-compliance with the LSS.

Two temperature sensors have discontinuous readings during the verification of the requirements R19 and R21. This is attributed to the same issue with the EGSE harness grounding by confirming proper functionality of the sensors in the later performance test.

With respect to the different temperature points for three of the four modules (see above), no difference can be detected between them. This means that the full temperature range poses no problem, even in the two temperatures that are seen critical.

E-Box thermal cycling test

The locomotion E-Box has been tested with eight locomotion engineering model (EM) motors housed in an aluminum block, as well as four sensor dummies, which were placed outside the TVC. The E-Box and the motor block were connected to two separate temperature-controlled plates (see Figure 10). This allows to cycle the temperature of the E-Box while maintaining the EM motors at $-25\,°\mathrm{C}$, which leads to the worst case motor currents, at all times.

During the test, the requirements from Table 8 had to be fulfilled. In order to validate the R28 requirement, all motor outputs of the locomotion E-Box have been powered and the motors in the motor block continuously operated for one hour in their nominal mode. The motor speed was set to $240\,\mathrm{rpm}$, which yields $4.12\,\mathrm{m}$ on Phobos in $1\,\mathrm{h}$, assuming no slip.

Table 9. TRP1 temperature setpoints of the locomotion E-Box QM thermal cycling test.

LSS state	min	max
non-OP	$-50\,°\mathrm{C}$	$65\,°\mathrm{C}$
OP	$-35\,°\mathrm{C}$	$65\,°\mathrm{C}$
Continuous Op	$0\,°\mathrm{C}$	

Table 10. Thermal requirements that are verified through analysis.

No.	Requirement
R29	Temperature gradient of contact surface at TRPs $< 3\,°\mathrm{C}$
R30	Heat flow through the E-Box thermal interface stays within given range

The TRP of the E-Box is located on the interface to the inner structure of the rover. In Table 9, the temperature set points for the thermal cycles can be seen.

During the locomotion E-Box thermal cycling test, all requirements from Table 8 are successfully verified without non-compliance.

Thermal analysis contribution to the verification

In addition to the tests, some of the thermal requirements are verified through thermal analysis. On LSS level, dedicated thermal models for the locomotion module and the E-Box were developed (see Figure 11). The analyses are performed based on the boundary conditions derived from the system level thermal analysis. They are used to verify that the predicted temperatures of the mechanical and electrical components inside the locomotion module and the E-Box are within their specified ranges. Of the requirements that were verified through analysis, two main ones are given in Table 10.

The interface between locomotion module and chassis is optimized for thermal isolation, which includes single stand-offs that form the actual interface instead of a contact all around the shoulder (see [2]). Due to this design, the temperature of the stand-offs is influenced by the surrounding temperature conditions which yields that the temperature uniformity of

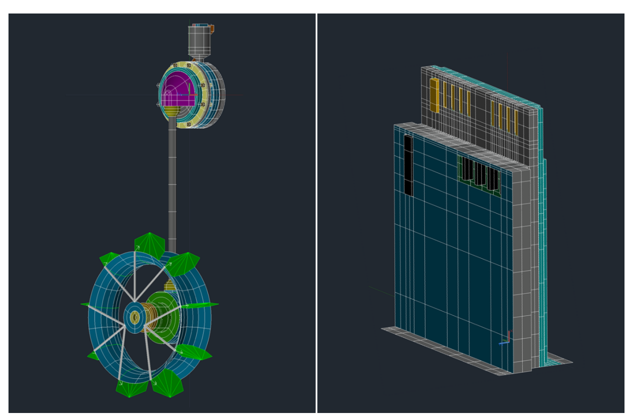

Figure 11. Thermal model of the locomotion module and the E-box.

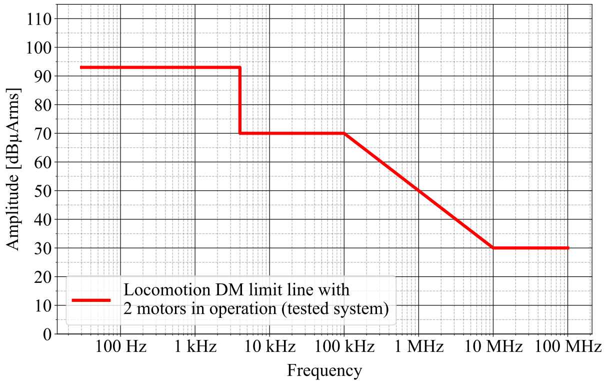

Figure 12. Tailored CE DM Locomotion Limit Lines.

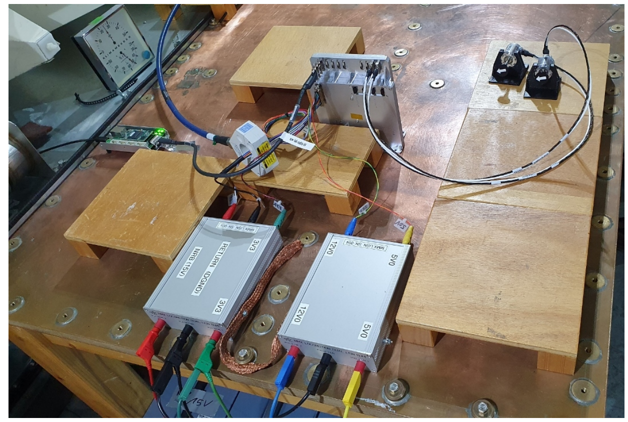

Figure 13. Hardware setup for EMC qualification testing.

R29 cannot be guaranteed. For the E-Box, the mounting surface is made of a solid aluminum alloy plate, which ensures compliance to R29 for the E-Box interface.

In terms of the heat flux requirement R30 for the E-Box interface, the heat flows from the E-Box to the rover inner structure during operation. This contradicts the requirement range but was not reasonable to design differently, since the major portion of the E-Box heat dissipation is rejected conductively.

The thermal analysis allowed, among many use cases, to identify this partial compliance and discuss them with the system analysis responsible. As a result, the identified thermal characteristics and related design are confirmed to be acceptable.

7. Electro-magnetic compatibility

The electromagnetic compatibility of the subsystems is crucial for the rover to function properly as an overall system. A malfunction or impairment of the individual systems among each other due to their electromagnetic properties must therefore be prevented.

Scope

The LSS has a potentially high level of interference due to its motors and the required power electronics. For this reason, attention was paid to reduce this interference emission to other systems based on the research on previous systems [5].

Conducted emission measurements have been carried out during the development phase with the EM E-Box and representative motor units. These measurement results provide a basis for the specification of the conducted EMC limits within the rover. The limits for the maximum emissions and minimum susceptibility for the LSS are based on the ECSS-E-ST-20-07C and are defined and tailored centrally together with the rover system responsible. Figure 12 shows the tailored limit lines for the Conducted Emissions (CE) in Differential Mode (DM).

The EMC qualification test campaign consists of 21 individual tests and measurements based on following setups:

- CE test, Current on power leads, Frequency Domain (FD), DM, from 30 Hz to 100 MHz, measured on power supply and return lines.
- CE test, Voltage on power leads, Time Domain (TD), DM, measured on 4 power supply against return line.
- CE test, Current on power bundle, FD, Common Mode (CM), from 10 kHz to 100 MHz, measured on power bundle.
- Conducted Susceptibility (CS) test, Current on power leads, FD, DM, from 30 Hz to 100 MHz, induced and measured on 4 power supply against return line.
- CS test, Current on power leads, FD, DM, from 50 Hz to 100 MHz, induced and measured on power bundle against case.
- CS test, Voltage on NRB power leads, TD, DM, Fast Spikes and Short Spikes, induced and measured in two polarities each on NRB supply against return line.

A true differential CE measurement cannot be performed due to the requirement on short cable lengths (0.3 m) between the line impedance stabilization networks (LISNs) and the DUT. Instead, a differential measurement was performed using only one supply line. Another challenge of testing the LSS is the increased number of power supply lines sharing one common return line. The power supply lines to be tested are the non-regulated bus (NRB), the 3.3 V, the 5.0 V, the 12.0 V and the return line. In addition, a custom LISN was designed, constructed and tested according to the expected power harness length of 1 m.

To ensure that the FM and FS E-Box behave in a very similar way as the QM, the EMC emission tests were also performed on them within the acceptance test campaign. The setup and results of the QM test serve as a basis for the EMC acceptance test in order to maintain comparability.

Conducted emission and susceptibility testing on QM

An external test house with an ECSS-E-ST-20-07C accredited chamber was required for these qualification tests. An overview of the test setup is shown in Figure 13.

The required components for the EMC test are:

- QM locomotion E-Box (DUT)
- Two LISNs to ensure cable properties on every power line
- SpaceWire to USB converter and representative cable
- Two representative motors and cables to load the E-Box
- Measurement equipment to measure the CE
- Signal generators for CS testing

During CE testing, the motors were driven at a constant speed and load profile to ensure a representative load on the E-Box. The emission test is terminated when the limit values

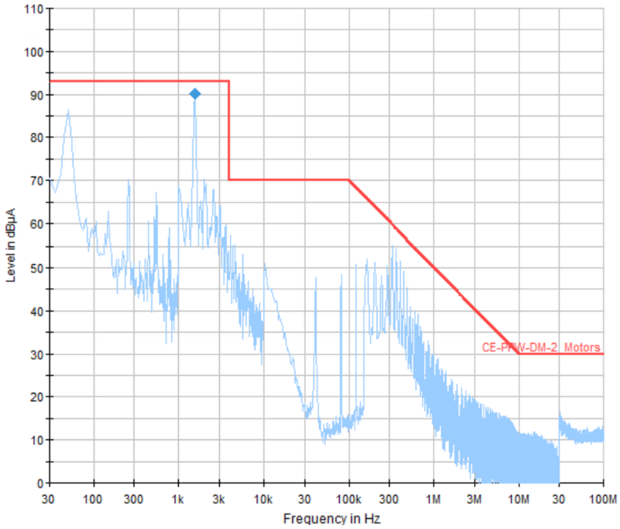

Figure 14. Emission limit (red) and measurement result (blue) of CE test on NRB power line in DM configuration within FD.

are exceeded or for the CS test in the event of recurring misbehavior (loss of communication or stalling of the motors). The test shows that the EMC requirements are met. One measurement result of the CE test on the NRB power line in DM configuration within FD is shown in Figure 14.

The peaks in the frequency range between 100 Hz and 3 kHz result from the motor movement and the dynamic current change. In the frequency range from 30 kHz up to 1 MHz, the peaks represent the effect of the hard switching behavior of the power inverters. The noise spectrum of the NRB current is therefore dominated by the motor operation and its required electronics. Susceptibility tests showed that the LSS is robust against the required limits on sinusoidal and pulse interference at the power inputs. Due to the common return line of all supplies of the LSS, an increased influence on the interference immunity of the supply line can be particularly excluded by the susceptibility tests.

8. PERFORMANCE TEST

As justified in Section 2, only one performance test is performed after the environmental tests to verify that all quantitative performance requirements for the LSS are met.

Scope

The key performance values of the LSS are determined by the uprighting sequence of the rover after being dropped on Phobos. It is possible that the wheels are buried in sand or are restricted by close-by boulders. Even under these conditions, the rover has to be able to lift itself up and point its solar panels towards the sun to be able to survive. To make sure that the required performance values are met, the LSS is subjected to the simulated environmental and operational loads in a TVC. Due to the long duration of the performance test, only the QM1 shoulder, that has seen the full thermal environment (cf. Section 6), is tested.

The main requirements that are verified with the performance test can be seen in Table 11. Note that the requirement R39 is verified by combining the backlash measurement of the performance test with a kinematic simulation. Details are given in the result subsection.

Table 11. Main performance test requirements.

No.	Requirement
R31	Power Consumption
R32	Speed range of the wheels
R33	Speed range of the legs
R34	Minimum torque of the shoulder output
R35	Minimum torque of the wheel actuators
R36	Torque sensor range and accuracy
R37	Backlash of the actuators
R38	Wheel and legs velocity accuracy
R39	Pose accuracy of the rover assuming flat ground

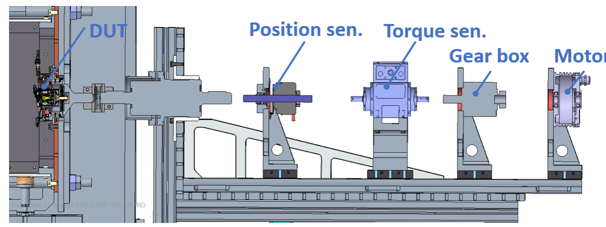

Figure 15. GSE setup of the performance test.

Performance test: setup and procedure

For the verification, the LSS is placed in a TVC which features a rotary feed through. The measurement equipment can therefore be placed outside the chamber in ambient condition (see Figure 15) which allows to use standard test equipment. The sensor suit consists of a Heidenhain ERN480 position and a Torquemaster TM306 torque sensor. Additionally, a load motor with a 1:5 gearbox is used to subject the DUT to the expected load torques. EtherCAT and USB buses are used to connect the test equipment to the test PC. The electrical power consumption and thermal behavior of the LSS is monitored with internal and external sensors.

The wheel and shoulder actuator are tested separately in favor of a feasible test setup, hence the LSS is mounted in two configurations. For testing the wheel actuator, the wheel itself is removed and replaced with an adapter that allows a connection to the rotary feed through with a standard coupling. For testing the shoulder drive, the entire leg is removed and several other adapters are used to fixate the DUT to the thermal regulator plate (see Figure 16).

The DUT is tested under seven different temperature cases as summarized in Table 12. The chamber is capable of

Table 12. Tested thermal cases during the performance test.

Cycle Nr.	TRP1* [°C]	TRP2 [°C]
1	ambient	ambient
2	+65	80
3	-65	-35
4	-65	-30
5	-65	-20
6	-65	-10
7	-65	-0

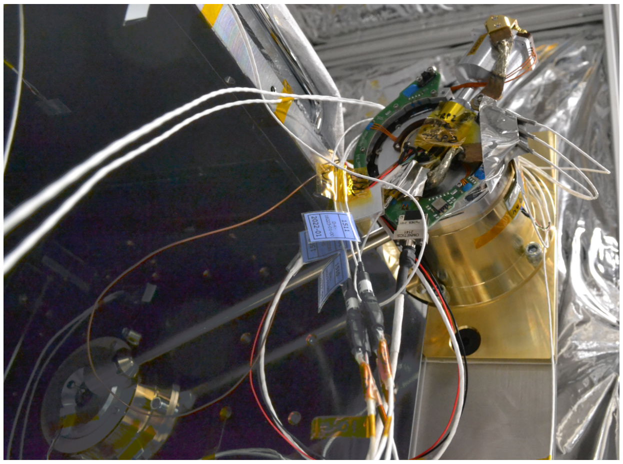

Figure 16. LSS configuration for testing of the wheel actuator. On the right, the shoulder module with several temperature sensors can be seen. On the left bottom is the wheel hub, which is connected to the mechanical feed-through shaft of the chamber instead of the wheel.

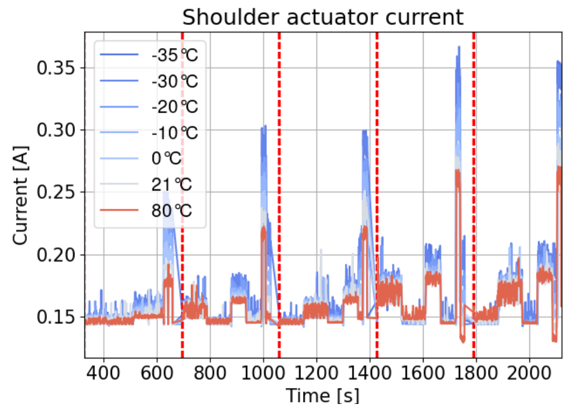

Figure 17. Shoulder actuator currents for the different TRP2 temperature cases. Left to right: $0\,\mathrm{N\,m}$, $2.5\,\mathrm{N\,m}$, $-2.5\,\mathrm{N\,m}$, $5\,\mathrm{N\,m}$, $-5\,\mathrm{N\,m}$, each case with the three speeds.

cooling down to $-65\,^{\circ}\mathrm{C}$, while the minimum TRP1 temperature according to the thermal environment is $-95\,^{\circ}\mathrm{C}$. Since the TRP1 is located on the outside of the rover body the representative internal temperature can be reached by removing the thermal separation ring between shoulder and chassis. An advantage of this measure is the shorter cool down time and decreased load on the thermal compressor. However, the leg and the driving end of the shoulder are tested with warmer temperatures. This leads to a lower sealing friction at the shoulder bearing and the wheel hub that has to be compensated for by applying an additional load with the load motor. This is done by extrapolating the beforehand measured friction to colder temperatures.

To compensate for the effects of the rotary feed through, its friction is identified under vacuum and with different speeds. It is added or subtracted to the applied load depending on the torque direction by the test sequence and data acquisition script. The only intervention by the test engineers is done for the no load motions, were the motor is decoupled to minimize the friction caused by the test equipment.

The wheel and shoulder actuators are tested up to a maximum load torque of $2.5\,\mathrm{N\,m}$ and $5\,\mathrm{N\,m}$, respectively. The load cycles include constant torques at three different speeds, ramping torques and a full load 400° turn at low speed. Before and after the cycles, a no load full rotation measurement is conducted to identify possible changes in behavior, such as degradation. The tested speeds are $0.039\,^{\circ}\,\mathrm{s}^{-1}$, $0.649\,^{\circ}\,\mathrm{s}^{-1}$ and $5.932\,^{\circ}\,\mathrm{s}^{-1}$ on the link side.

Performance test: results

In Figure 17 one can see the impact of the temperature on the shoulder actuator current. The constant load cases with the three different speeds are shown. In previous actuator designs, the increasing viscosity of the HD gearing lubrication and the thermal influence on the small parts resulted in high current draw at temperatures below $-20\,^{\circ}\mathrm{C}$ [6]. The data shows that the two stage gearing solved this problem. The actuator stayed below its maximum allowed current (already with a margin of three as explained in Section 3) of $1.5\,\mathrm{A}$ by far in all cases.

Due to the high friction of the sealing in the LSS, it was expected that the torque sensor accuracy requirement of $0.05\,\mathrm{N\,m}$ would not be met in the assembled LSS. There was no need identified by the rover responsible since the torque sensor is only meant to detect blockage. This usage does not pose any accuracy requirement to the torque sensor, which is why the deviation is acceptable. The torque data recorded during the ramping torque sequence confirmed the accuracy non-compliance, as can be seen in Figure 18. Only the data where the internal sensor is not saturated is shown. Especially in the generative operation one can see the constant friction for the warm and cold cases, with are measured around $0.2\,\mathrm{N\,m}$ and $0.4\,\mathrm{N\,m}$ respectively.

Furthermore, the speed accuracy requirement could not be verified with the available measurements. The accuracy is defined relatively to the medium speed in percent which makes it very sensitive to deviations during low speeds. The communication between GSE and the DUT is not set up as real-time compliant, therefore the noise on the position measurement leads to a fail of this requirement. Since this is an issue of the GSE setup and the speed accuracy is met at higher speeds, the deviation is accepted.

All other requirements are met including all output speeds, output torques, temperatures and backlash of the LSS.

For the rover pose accuracy requirement R39, the leg backlash measurement was combined with the worst case tolerance chain to get to an error of the leg angle knowledge. This is then used in a kinematic simulation by assigning the possible leg angle error in different combination to the four legs and simulating the resulting pose of the rover. The result is a 3σ error of $\pm 4.4\,\mathrm{mm}$ and an orientation accuracy of 1.63° for a workspace of 0°-15° and $10\,\%$-$90\,\%$ height. These values are well within the requirement.

9. LIFE TEST

The life test aims to confirm that the functionality of the LSS will still be within the requirements after the movements performed during assembly, acceptance tests and the actual mission.

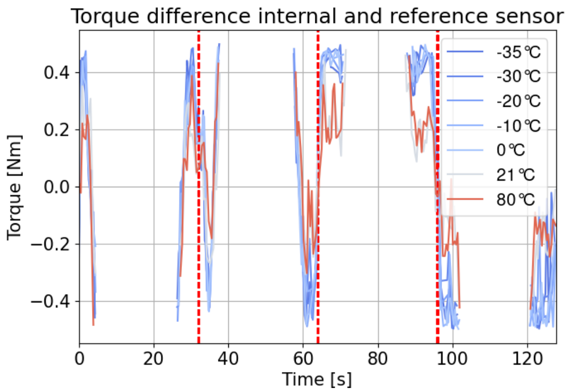

Figure 18. Torque difference during ramping torque sequence. Left to Right: LSS in motor operation, positive and negative direction, LSS in 'generative' operation positive and negative direction.

Table 13. Main life test requirements.

No.	Requirement
R40	The legs have to perform three full turns back and forth for uprighting.
R41	The legs have to be moved by $40°$ back and forth forty times for sun alignment.
R42	The rover has to drive one hundred meters.
R43	Continuous operation of locomotion for one hour (for the module; see Section 6 for the E-Box counterpart).

Scope

As defined in [7], the life test is performed under representative thermal conditions with motion speeds, profiles and loads representative to operational conditions.

The life of the LSS is defined by the sum of flight model movements, which includes subsystem acceptance test, system tests and, of course, the mission itself. This sum is multiplied by a factor four as defined in ECSS for space mechanisms (see [7]). The moves related to the nominal mission are estimated based on the requirements of the mission and the most important are listed in Table 13. Test plans for acceptance tests of the LSS and system tests are used to predict the sum of movements on ground. Altogether, this results in more than 2000 full rotations of the legs with over 1000 direction changes and almost 700 full rotations of the wheels with more than 300 direction changes.

It is the purpose of the life test to demonstrate that the performance of the system is not degraded so much as to drop out of the specifications during the simulated life. Hence, the evaluation of the life test is done by comparing the key performance indicators of the LSS before and after the life test. The sequence and measurement of the performance test (see Section 8) are used.

Test setup and procedure

The test setup of the performance test (see Section 8) is well suited for the life test and is used without modifications.

The expected movement patterns of the flight model are accounted for by performing repetitive small movements and direction changes (like during sun alignment) as well as full turns and longer movements (like during uprighting and driving). In order to consider the demanding thermal conditions on Phobos while keeping the test duration manageable, three groups of thermal conditions are defined and the movements are spread among these groups.

a) Minimum temperature with cold start: Worst case scenario for drive train and electronics where the movement starts at the minimum operational temperature (i.e. TRP2 at $-35\,°C$). Due to the self-heating during operation, a wait time is introduced between the movements to let the LSS temperatures cool back down to the minimum operational temperature. Since the cold start is regarded as the critical aspect for this thermal condition, especially short movements are performed in this mode.

b) Minimum temperature with continuous movement: Wheel and leg motors are driven continuously starting at the minimum operational temperature of the LSS.

c) Maximum temperature with continuous movement: Wheel and leg motors are driven continuously starting at the maximum operational temperature of the LSS (i.e. TRP2 at $80\,°C$).

Test results

Figure 19 shows the motor phase currents before and after the life test of a leg motor during a movement with the same load, speed and environmental conditions. A slightly lower motor phase current can be observed after the life test which can be explained by better run-in gear boxes. No loss of performance could be identified between the performance test before and after the life test, neither for the shoulder nor for the wheel. There is no measured degradation trend of the system. A visual inspection after completion of the life test showed some wear on the gears of the wheels, which, however, does not impair functionality. The life test was therefore concluded successful.

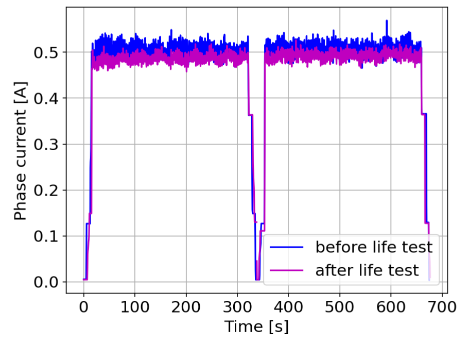

Figure 19. Comparison of motor phase currents of a leg motor before and after the life test.

10. SOFTWARE FUNCTIONAL TEST

The software functional test (SFT) concerns the locomotion software partition (LOCO) that runs on the on-board computer (OBC) of the rover. This test was performed with the most up-to-date LOCO version in summer 2022, however, it will be repeated with coming software updates from system and LSS side.

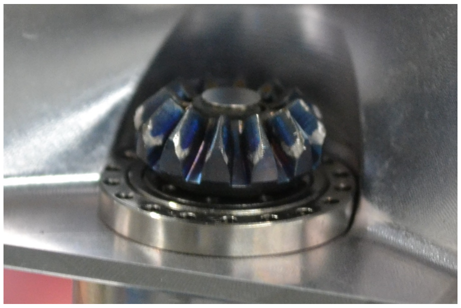

Figure 20. Wear at gears.

Table 14. Main software test requirements.

No.	Requirement
R44	be able to command the driving capabilities via the software, in particular the different locomotion modes and the direct motor control, see [8]
R45	provide safety functions, fault detection, isolation and recovery, including overload detection
R46	stay within the given computational resources and communicate with the desired frequency
R47	have properly defined interfaces to the OBC and the E-Box, in particular correctly send commands and reliably receive housekeeping data
R48	be able to adjust the parameters, e.g. have different leg range limits before and after the solar array deployment

Scope

The SFT is performed at DLR in Oberpfaffenhofen and its purpose is to confirm that LOCO on the OBC implements the required features and can perform them on representative hardware. These main requirements for software testing are listed in Table 14.

Eleven test sequences are defined to test all of the requirements and a total of 25 pass/fail criteria are specified.

Setup

The test campaign is mainly conducted on hardware, except for a part of the failure detection, which is performed in a software-in-the-loop (SIL) simulation [9] to not having to introduce actual failures in the hardware.

The test equipment for the hardware-in-the-loop tests includes:

- an EM of the MMX OBC and PCDU, provided by CNES
- the QM locomotion E-Box
- EM locomotion modules including motors and sensors
- harness to connect everything

Further supply equipment includes:

- a PC simulating the ground module, i.e. for sending telecommands and receiving telemetry
- a TMTC brick (provided by CNES) between the ground-PC and the OBC to convert the telemetry and telecommands into the according data format
- a laboratory power supply to replace the rover's battery
- a camera to document the movements of the motors.

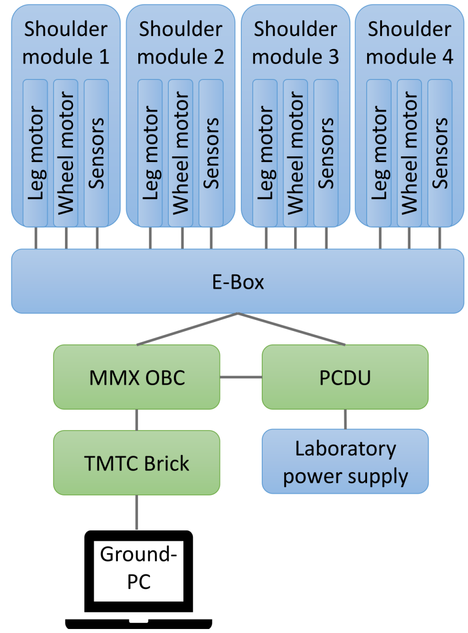

Figure 21. Setup of the software functional test. Equipment provided by CNES is depicted in green, DLR/LOCO hardware in blue.

The test setup is shown in Figure 21.

Procedure

For testing the software, the LOCO source code is cross-compiled for XtratuM on an ARM target. The software is then loaded onto the OBC. Each single test sequence has its own test script which is then executed. After the test sequence ended, the telemetry data is exported and analyzed in a post-processing procedure. This allows to assess if a previously defined pass/fail criterion is met or not.

To test elements of the software that are not yet fully supported by the remaining OBC software or that may be dangerous to the hardware the SIL setup is used. This setup is based on an adapted version of the MMX robotics simulation setup presented in [9]. The physical simulation is extended by two main components: A representation of the interface to the rest of the OBC and a simulation of the E-Box. By directly replacing the interfaces to both components in the LOCO source code and then compiling the LOCO source code as a library, it can be used seamlessly in the SIL setup. This setup has the additional benefit of no synchronization issues. Sequences of telecommands can be defined in Lua scripts which are then parsed by the OBC software simulation. Both the E-Box and OBC simulation software are developed to mimic the behavior document for both components. Critical benefits of this setup are a straightforward solution to induce failure in the simulated E-Box and test the LOCO software's expected behavior as well as a safe method to test features like collision detection.

Results

The SFT is not only used for verification but also as an integration test campaign, which revealed last small bugs that could be solved immediately. The full SFT is ultimately performed with a dedicated release version of the software to verify all requirements. With that release version, 24 out of 25 pass/fail criteria succeeded, the remaining non-compliance (part of R47) is formulated as NCR and will be tackled with the next software release.

Since the full MMX Rover software is still under development, interfaces can still change and software is continuously updated. The procedure of the software functional test will be repeated with future releases of LOCO, including the flight release, to validate that all requirements are still fulfilled.

11. Components verification

The spin-in of COTS is an important topic for the locomotion subsystem. Due to space and weight requirements, the drive unit utilizes two different COTS parts for the drive electronics: A BLDC motor driver DRV8332 from Texas Instruments [10] and an industrial Hall effect sensor TLE4945L from Infineon [11]. Furthermore, a Gyroscope from Silicon Sensing CRM200 [12] and a military 3 axis MEMS accelerometer from Analog Device [13], are utilized during the landing on Phobos.

This section comprises these component-level qualification tests or analysis, namely

- radiation and deep temperature tests of EEE components,
- dust break-in test of the shoulder sealing concept,
- outgassing of an epoxy resin glue.

Radiation and deep temperature tests of EEE components

The requested TID robustness as well as the test results are shown in Table 15. For each of the selected COTS parts, the margin between the needs and the performance is larger than the factor of 2.5. After irradiation with the listed total dose, all parts were fully operational.

Table 15. TID performance of the used COTS parts

Device	Location	TID needed	Test result
DRV8332	Loco E-Box	5 kRad	50 kRad(Si)
CRM200	Loco E-Box	5 kRad	16.7 kRad(Si)
TLE4945L	Loco modules	10 kRad	25.6 kRad(Si)
ADXL356-EP	Loco modules	10 kRad	29.3 kRad(Si)

Due to the tight schedule of the project, and the fact that the Gyroscope CRM200 and the accelerometer ADXL356-EP are used only for a short period during the landing on Phobos, the extent of the spin-in procedure was reduced. Only TID tests were conducted for these devices, performed at the Helmholtz-Zentrum Berlin Wannsee [14] at room temperature. After the up-righting of the rover, the power supply of these two devices is switched off, therefore no particle based error is expected. In addition, both devices are located in the isolated, warmer locomotion E-Box, which eliminates the need of a component temperature test that was performed for the Hall effect sensor TLE4945L. These devices are located in the outer area of the rover and they must withstand extreme temperature ranges of -75°C to +85°C (non operational). This goes beyond the temperature range of industrial electronics and space grade electronics.

Details on the qualification procedure of the BLDC motor driver DRV8332 can be found at [15], and of the Hall effect sensor TLE4945L at [16].

Table 16. Compliance levels after forced outgassing.

Duration	TML[%]	RML[%]	CVCM[%]	Compliance
0h	2.18	1.71	0.0	FAILED
50h	1.4	0.9	0.0	PASSED
100h	1.31	0.81	0.0	PASSED

Glue outgassing

The epoxy resin DELO DUOPOX SJ8665 is used primarily for potting and coating of motor-related components, such as stators, windings and the Hall sensor PCB. According to the supplier information and MAPTIS database for materials and processes, the glue is not conformal with the required outgassing limits of the ECSS-Q-ST_70-02C. The recovered mass loss (RML) is required to be $< 1.0\,\%$ and collected volatiles condensable material (CVCM) $< 0.1\,\%\%$, whereas the glue's properties can be seen in Table 16. To exploit the resin's preferable mechanical properties as well as the broad experience of use at the institute, the decision was made to qualify the glue further. Therefore, besides curing according to the manufacturer's manual, the samples needed to be treated with additional forced outgassing. For that reason, two samples of cured glue were prepared. The resin was mixed and prepared according to the manufacturer's manual and casted into specially designed outgassing PTFE-mold onto an 16μm thick aluminum-sheet substrate to form a $150\,\mathrm{mm}$ x $150\,\mathrm{mm}$ x $3\,\mathrm{mm}$ solid block. The outgassing was performed for $50\,\mathrm{h}$ and $100\,\mathrm{h}$ at $80\,°\mathrm{C}$ each. After outgassing, the block was demolded, cleanly packed and transported to a DLR test facility in Bremen, where the outgassing analysis was performed on the Micro-VCM Testbench.

The test shows that the performed procedure reduced outgassing values effectively and yields compliance already after $50\,\mathrm{h}$ curing at $80\,°\mathrm{C}$, see Table 16. A respective curing step is thus added to the procedure for the QM and FM.

Dust break-in test

The dust break-in test was conducted to verify the functionality of the seals in the shoulder modules as well as in the wheels. This was qualified with EM hardware since the sealing concept did not change between EM and QM/FM, thus it is described in [2] and only briefly summarized here for completeness. A shoulder seal of the MMX Rover was exposed to a dusty environment and operated (see Figure 22). During the test time, the seal was driven in both directions, while excessively trickling sand through a funnel onto the shoulder unit. The used sand mixture contained grain sizes from $40\,\mu\mathrm{m}$ to $6\,\mathrm{mm}$.

After the test, a post inspection of the shoulder sealing was performed by dismounting and checking whether dust or sand trespassed the sealing. As expected, only a small amount of fine sand came out of the first of two sealing stages by gently shaking the hardware and almost no sand was found behind the second stage. Since the amount of sand that protruded the sealings is not critical and the unit was actuated during the test without any problems or jamming, the dust break-in test is successful.

Wheel side-slip analysis

The wheel design is required to allow side slip angles of about $45°$ without excessive sinkage for a distance of $0.1\,\mathrm{m}$. This side slip ability is needed since the rover does not have

Figure 22. Dust break-in test setup.

steering actuators but turns through differential wheel speeds on the left/right side. Curves or point turns therefore lead to side-slip angles of up to about $45°$, depending on the curve radius as well as the leg angles and thereby the height setting of the rover. As the terrestrial gravity increases the density of the regolith, and thereby lowers the wheel sinkage, a test lab cannot provide realistic conditions on Earth. Therefore, the verification is performed by an analysis with the Discrete Element Method. In order to keep simulation times manageable in the given time frame, a single wheel is simulated driving straight while having a $45°$ steering angle. Bulldozing is much more evident in side slip than in point turn, as in the latter the wheel moves on a circular trajectory and avoids parts of the bulldozed heap for further movement. Thus, as bulldozing is considerably higher in this situation than in a real point turn, the test is considered a worst case scenario. The FM wheel design was compared to a conventional rover wheel design (outward bent wheel rim) in order to verify that it performs as well as the conventional one in point turns.

In addition to the detailed simulation campaigns, point turn tests with a terrestrial prototype are performed to strengthen the findings of the analysis.

The reduced overall turning resistance of the rover by the asymmetric design (cf. [17]) of the FM wheel is confirmed by the analysis. Both, the conventional wheel as well as the FM wheel, show slip values of less than $80\,\%$ for $15\,\text{cm}$, as shown in Figure 23, which is longer than the required $10\,\text{cm}$.

Thus an asymmetric wheel design is the solution to the problem at hand, as it shows similar performance in side slip simulation (i.e. point turn), compared to a conventional wheel, but outperforms it in any other situation tested.

12. Summary & Outlook

The qualification campaign of the LSS was completed in June 2022. Some minor issues were revealed but only the failure of the foil potentiometer in cold temperature required a design change of the FM. Due to the originally three sources of the leg angle information, this loss of one of the potentiometers per shoulder does not yield a loss of function or performance and the leg angle is still sensed redundantly. This failure can be attributed to the short development time and very few test and design iterations that were feasible before the manufacturing of the QM and FM hardware. The investigation is ongoing and will be continued until a conclusive result is found to learn for future projects.

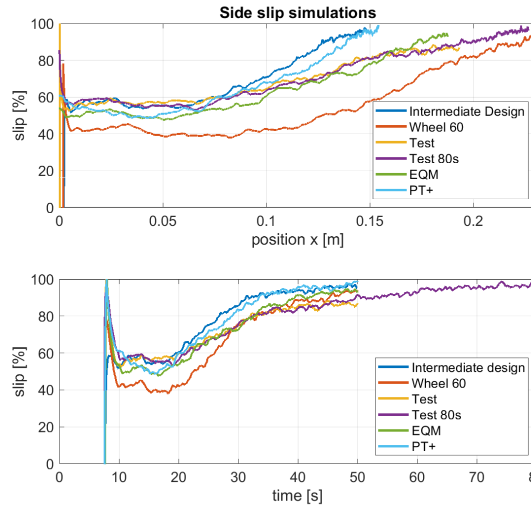

Figure 23. Side slip analysis results.

In a qualification review, the MMX Rover management, the verification responsible, the system engineers and the product assurance evaluated the results of the LSS qualification campaign. In the final report, the LSS was concluded to be qualified for the MMX mission and released for higher-level integration. The planned rover level vibration test is, however, particularly important for the LSS since there remains a risk that the qualification loads for the LSS campaign were not conservative enough.

During the assembly, integration and testing of the MMX rover, some tests are requested by the LSS to verify nominal functionality of all interfaces. These tests will be performed within the second half of the year 2022 and the whole MMX rover will be shipped to Japan in 2023.

Acknowledgments

The authors acknowledge the work of the whole locomotion team as well as the valuable recommendations from other MMX project members and external reviewers. It has been an incredible team effort to get the entirely newly developed locomotion subsystem from the first prototypes in early 2020 to a fully qualified subsystem and accepted FM hardware in only two and a half years.

References

[1] H.-J. Sedlmayr, S. Barthelmes, R. Bayer, W. Bertleff, M. Bihler, F. Buse, M. Chalon, D. Franke, F. Ginner, V. Langofer, R. Lichtenheldt, T. Obermeier, A. Pignède, J. Reill, and J. Skibbe, "MMX – Development of a Rover Locomotion System for Phobos," in *Proceedings of the IEEE Aerospace Conference*, 2020.

[2] S. Barthelmes, T. Bahls, R. Bayer, W. Bertleff, M. Bihler, F. Buse, M. Chalon, F. Hacker, R. Holderried, V. Langofer *et al.*, "MMX rover locomotion subsystem - development and testing towards the flight model," in *Proceedings of the IEEE Aerospace Conference*.

[3] V. Langofer, R. Bayer, and A. Kolb, "MMX Locomotion Subsystem: mechanics for extraterrestrial low gravity drive," in *Proceedings of the IEEE Aerospace*

Conference, 2023.

[4] (2022) MIL-STD-883L, Department of Defense Test Methode Standard: Microcircuits. [Online]. Available: http://everyspec.com/MIL-STD/MIL-STD-0800-0899/MIL-STD-883L_56323/

[5] S. Moser, “Reverse EMI behaviour of DC-DC converters,” in *proceedings of the ESA Workshop on Aerospace EMC (Aerospace EMC)*. IEEE.

[6] M. Chalon, M. Maier, W. Bertleff, R. Beyer, Alexander Bayer, W. Friedl, P. Neugebauer, T. Obermeier, H.-J. Sedlmayr, N. Seitz, and A. Stemmer, “Spacehand: a multi-fingered robotic hand for space,” in *ASTRA 2015*, 2015.

[7] European Cooperation for Space Standardization (ECSS), “ECSS-E-ST-33-01C-Rev.2 - Sace engineering - mechanisms,” 2019.

[8] J. Skibbe, S. Barthelmes, and F. Buse, “Locomotion control functions for the active chassis of the mmx rover,” in *2021 IEEE Aerospace Conference (50100)*, 2021, pp. 1–9.

[9] F. Buse, A. Pignède, T. Simon, J. Bertrand, S. Goulet, and L. Sandra, “Mmx rover simulation - robotic simulations for phobos operations,” in *2022 IEEE Aerospace Conference*, 2022.

[10] (2021) Texas Instruments Incorporated, 3-Phase Motor Driver. [Online]. Available: https://www.ti.com/product/DRV8332

[11] (2021) Infineon Technologies AG, Linear Hall Sensors. [Online]. Available: https://www.infineon.com/cms/en/product/sensor/magnetic-sensors/magnetic-position-sensors/linear-halls/

[12] (2022) Silicon Sensing Systems Limited, Gyroscope. [Online]. Available: https://www.siliconsensing.com/products/gyroscopes/crm-pinpoint/

[13] (2022) Analog Devices Incorporated, 3-Axis Accelerometer. [Online]. Available: https://www.analog.com/en/products/adxl356.html

[14] (2021) Helmholtz Zentrum Berlin Wannsee, Cobalt-60-Source. [Online]. Available: https://www.helmholtz-berlin.de/forschung/oe/be/protonentherapie/index_de.html

[15] H.-J. Sedlmayr, A. Beyer, K. Kunze, and M. Maier, “Radiation test of a BLDC motor driver component,” in *2018 IEEE Radiation Effects Data Workshop*, 2018.

[16] H.-J. Sedlmayr, S. Barthelmes, F. Hacker, K. Kunze, and M. Maier, “Upscreening of infineon hall effect sensors for the mmx rover locomotion subsystem,” in *2022 RADECS Data Workshop*, 2022.

[17] L. Stubbig and R. Lichtenheldt, “Optimizing the shape of planetary rover wheels using the discrete element method and bayesian optimization,” in *VII International Conference on Particle-based Methods – Particles*, 2021.

BIOGRAPHY

Stefan Barthelmes *received his Dr.-Ing. degree in Electrical Engineering at TU Darmstadt and his B.Sc. and M.Sc. degree in Mechanical Engineering from TU München. He is currently working as a researcher at the Institute of System Dynamics and Control of the German Aerospace Center (DLR). His main research focus is model-based chassis control and simulation model development of planetary exploration rovers. Within the MMX mission, he is responsible for the rover’s locomotion subsystem.*

Ralph Bayer *received his Master of Science (M.Sc.) in Mechanical Engineering from the Regensburg University of Applied Sciences, Germany, in 2011 and joined the German Aerospace Center (DLR) in 2010. He was a member of the development team of the space qualified force feedback joystick used for the KONTUR-2 ISS-to-ground telemanipulation experiments in 2015-2016, as well as the METERON SUPVIS Justin ISS-to-ground telerobotic experiments in 2017–2018. He currently serves as the lead thermal engineer at DLR’s Institute of Robotics and Mechatronics. Mr. Bayer plays a key role in the thermal design of the MMX locomotion subsystem.*

Wieland Bertleff *received his Dipl.-Ing. (FH) from the University of Applied Sciences in Heilbronn in 2002. He started his work at the German Aerospace Center at the Institute of Robotics and Mechatronics in Oberpfaffenhofen and studied, in parallel, Electrical Engineering. 2007 he received his M.Sc. degree in Electrical Engineering from the University of Applied Sciences, Munich. Wieland is involved in the development and design of force and torque sensors for robotic systems. He also contributed in the robotic mission “ROKVISS” in the field of friction identification. For the MMX mission, he focuses on qualification and test campaigns of the space hardware.*

Markus Bihler *received his M.Sc. degree in computer science from the University of Applied Science Augsburg, Germany in 2015. Since then, he has been with the German Aerospace Center, Institute of Robotics and Mechatronics, working in the field of FPGA development. Since October 2017, he is group leader for digital electronics. Within the MMX mission, he is responsible for the firmware in the central electronic box of the rover’s locomotion subsystem.*

Fabian Buse *received his Dr.-Ing. degree in Aerospace Engineering from Tōhoku University and his B. Sc. and M. Sc. from RWTH Aachen University. Since 2015, he has been Research Associate at the Institute of System Dynamics and Control (SR). His research interests are in terramechanics for planetary rovers. He is the lead engineer of the DLR Terramechanics Robotic Locomotion Lab (TROLL) and is leading the rover simulation for the MMX Rover project.*

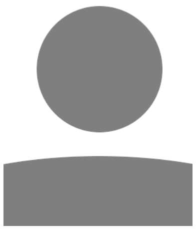

Maxime Chalon *received his Dr.-Ing. degree in Control Theory at Mines ParisTech and his B.Sc. and M.Sc. degree in Mechatronics Engineering from Ecole des Mines d'Ales. He is currently working as a research associate at the Institute of Robotics and Mechatronics of the German Aerospace Center (DLR). His main research focus is space robotics. Within the MMX mission, he is responsible for the rover's system engineering and partially the locomotion system engineering.*

André Fonseca Prince *received his MSc. degree in Mechatronics Engineering from the Politecnico di Torino, Italy in 2020. Since then, he has been working in the Robotics and Mechatronics Institute at the German Aerospace Center (DLR) as Mechatronics engineer. He has contributed to the Power Management and Data Handling systems of the Moon analogue multi-robot project ARCHES since 2020 and, within MMX, to the firmware in the central electronic box of the rover's locomotion subsystem. His fields of interest are electronics communication, motor control, and power electronics within robotic planetary exploration.*

Franz Hacker *received his Dipl.-Ing. degree in Electrical Engineering and Information Technology from TU München. Since 1994, he works as research associate at the German Aerospace Center, Institute of Robotics and Mechatronics. His main research focus is the design and optimization of analog electronics and sensors used for robotic systems in terrestrial and space applications. Within the MMX mission, he is responsible for the central electronic box of the rover's locomotion subsystem.*

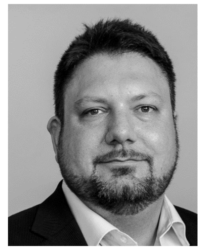

Günther Geyer *received his degree in business administration from the University of Applied Science Ingolstadt in 2007. Since 2020 he has been with the German Aerospace Center (DLR), Institute of Robotics and Mechatronics. His main focus is on maintenance and further development of the quality management system (ISO 9001).*

Cynthia Hofmann *received her Dipl.-Ing. (BA) degree in Electrical Engineering from the university of cooperative education in Ravensburg in 2004. She works at the German Aerospace Center (DLR), Institute of Robotics and Mechatronics as a systems engineer since July 2019. Her main focus is in the fields of terrestrial assistance robotics. She supported the MMX mission with technical management by planning the ressources for the qualification and acceptance tests of the rover's locomotion subsystem.*

Roman Holderried *received his B.Eng. from University of Applied Science in Kempten and his M.Sc. from University of Applied Science Munich, both in Electrical Engineering. Since 2019, he has been with the German Aerospace Center, Institute of Robotics and Mechatronics. His main research interest is the design and implementation of control algorithms for electrical drives in terrestrial and space robotics applications. Within the MMX project, he contributed to the development of the drive controllers of the locomotion subsystem and was involved in the test design of the qualification test campaign.*

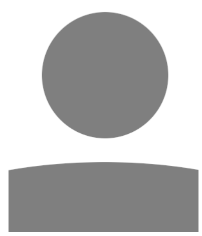

Alexander Kolb *graduated as a Dipl.-Ing. in Mechatronics from the University of Innsbruck, Austria in 2019. Since then, he has been working at the German Aerospace Center (DLR), Institute of Robotics and Mechatronics as a mechanical engineer. He did his first work in the field of medical robotics, transitioning to space domain in 2020. His research focus lies on the optimization of electromechanical actuators.*

Erich Krämer *received his Dipl.-Ing. (FH) in Precision Engineering at University of Applied Sciences Munich. Since 1990 he is working as a Design Engineer at the Institute of Robotics and Mechatronics of the German Aerospace Center (DLR). His main research focus is the mechanical design for space qualified robotic systems such as EuTEF, ROKISS, ConeXpress-OLEV, Dexhand, DEOS or CAESAR.*

Viktor Langofer *received the degrees of B.Sc. and M.Sc. from Technische Universität Kaiserslautern. Since 2017, he has been Research Associate at the German Aerospace Center (DLR), Institute of Robotics and Mechatronics. His main area of activities are research in compliant and tendondriven mechanisms in humanoid robotics, as well actuators design for space applications. He is responsible for the mechanical design of the locomotion subsystem of the MMX Rover.*

Roy Lichtenheldt *received his Dr.-Ing. degree in Mechatronics at TU Ilmenau. He is currently working as a research associate at the Institute of System Dynamics and Control of the German Aerospace Center (DLR). His main research interest is terramechanics and innovative locomotion systems. Currently he is leading a group developing the Scout rover to explore lunar and martian lava tubes by 2030. Within the MMX mission, he leads the development of the rover's wheels.*

Sascha Moser *received his M.Sc. and B.Sc. degree in Electrical Engineering and Information Technology from TU München. Since 2016, he has been with the German Aerospace Center, Institute of Robotics and Mechatronics. His main research focus is the design and optimization of power and analog electronics, power management and electromagnetic compliance (EMC) used for robotic systems in terrestrial and space applications. Within the MMX mission, he is responsible for EMC design and tests of the rover's locomotion subsystem.*

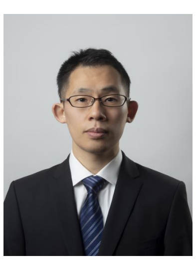

Kaname Sasaki *received his Master degree in Aerospace Engineering from Tokyo University, Japan. Since 2013 he works at the department of Mechanics and Thermal Systems of the DLR Institute of Space Systems in Bremen, Germany. He contributed to the development and operation of the asteroid lander MASCOT and the DLR payload HP³ as part of the NASA/JPL Mission INSIGHT. Currently, he is involved in the thermal design and analysis of the locomotion subsystem in the MMX Rover project.*

Hans-Juergen Sedlmayr *received his Dipl.-Ing. degree in Electrical Engineering from the University of Applied Science Munich in 1992. Since 2001, he has been with the German Aerospace Center, Institute of Robotics and Mechatronics. His main research focus is in the field of radiation testing of electric and electronics parts and embedded software development inside robots for terrestrial and space applications. Within the MMX mission, he is responsible for quality assurance of the rover's locomotion subsystem.*

Juliane Skibbe *studied Mathematics at the University of Wuerzburg and the Université d'Orléans. After finishing her Master's degree in 2018, she started working as a research associate at the Institute of System Dynamics and Control of the German Aerospace Center (DLR). Today, she leads the MMX Locomotion Software team. Her main research focus is on developing locomotion control algorithms for rover for planetary exploration, in particular fault detection, isolation and recovery.*

Bernhard Vodermayer *received his degree computer science in 2006 at the Technical University of Munich while he has been scientifically associated with the Institute of Robotics and Mechatronics since 2004. Till 2012, he played a key role in the development and the technology transfer of the DLR's left ventricular heart assist device DLR-LVAS. Since 2010, he is scientifically related to space based technologies for safe robotic docking and energy management of wheeled, autonomous vehicles for planetary exploration. His research interests are in the field of novel, future emerging technology based actuator and sensor systems, polymer-based systems and related production processes, space technologies, mobile space robotics as well as biomedical devices and active implants. Within MMX he is responsible for the development and qualification of the rotational sensors used in the locomotion subsystem as well as testing and AIT processes.*